Available online at www.sciencedirect.com
SCIENCE DIRECT®
Applied Surface Science 235 (2004) 221–226
applied surface science
www.elsevier.com/locate/apsusc

Photon reflectivity distributions from the LHC beam screen and their implications on the arc beam vacuum system

N. Mahne[a,1], V. Baglin[b], I.R. Collins[b], A. Giglia[a,1], L. Pasquali[c,2], M. Pedio[a,1], S. Nannarone[a,c,1,2], R. Cimino[b,d,*]

[a]*TASC-INFM, SS 14, Km 163.5, Basovizza, Trieste, Italy*
[b]*CERN CH-1211, Geneva 23, Switzerland*
[c]*Università di Modena e Reggio E.-41100, Modena, Italy*
[d]*LNF-INFN 00044, Frascati, Italy*

Available online 28 July 2004

Abstract

In particle accelerators with intense positively charged bunched beams, an electron cloud may induce beam instabilities and the related beam induced electron multipacting (BIEM) can result in an undesired pressure rise. In a cryogenic machine such as the large hadron collider (LHC), the BIEM will introduce additional heat load. When present, synchrotron radiation (SR) may generate a significant number of photoelectrons, that may play a role in determining the onset and the detailed properties of the electron cloud related instability. Since electrons are constrained to move along field lines, those created on the accelerator equator in a strong vertical (dipole) field cannot participate in the e-cloud build-up. Therefore, for the LHC there has been a continuous effort to find solutions to absorb the photons on the equator. The solution adopted for the LHC dipole beam screens is a saw-tooth structure on the illuminated equator. SR from a bending magnet beamline at ELETTRA, Italy (BEAR) has been used to measure the reflectivities (forward, back-scattered and diffuse), for a flat and a saw-tooth structured Cu co-laminated surface using both white light SR, similar to the one emitted by LHC, and monochromatic light. Our data show that the saw-tooth structure does reduce the total reflectivity and modifies the photon energy distribution of the reflected photons. The implications of these results on the LHC arc vacuum system are discussed.

PACS: 29.27.Bd; 78.40. q

Keywords: Beam dynamics; Collective effect and instabilities; Absorption and reflection spectra: visible and ultraviolet

1. Introduction

The LHC design will provide two counter-circulating proton beams with colliding energies of nominally 14 TeV in the centre of mass, requiring superconducting bending magnets operating in super-fluid helium at 1.9 K. In order to reduce the cryogenic power consumption at 1.9 K in the arcs, the heat load induced by the beam will be intercepted on a beam screen, which

* Corresponding author. Present address: LNF-INFN 00044, Frascati, Italy. Tel.: +39 06 9403 2358; fax: +39 06 9403 2304.
E-mail address: roberto.cimino@lnf.infn.it (R. Cimino).
[1] TASC-INFM, SS 14, Km 163.5, Basovizza, Trieste, Italy.
[2] Università di Modena e Reggio E.-41100, Modena, Italy.

0169-4332/$ – see front matter © 2004 Elsevier B.V. All rights reserved.
doi:10.1016/j.apsusc.2004.05.271

operates between 5 and 20 K. In the arcs of the machine, desorbed molecules will be pumped through the pumping slots, distributed along the length of the beam screen, onto the surrounding cold bore held at 1.9 K.

The emitted synchrotron radiation (SR) from the circulating protons, with a critical energy of 44.1 eV, is a major consideration for the design of the vacuum system. Its radiated power, induces a heat load of 0.2 W/m at 7 TeV per beam and may (i) stimulate gas desorption of weakly and tightly bound gases from the walls of the vacuum system either directly by photons or mediated by electrons [1,2], (ii) create photoelectrons [3] which, at nominal LHC conditions, can be accelerated, to an average energy of 90 eV [2,4,5], towards the opposite wall by the positive space charge of the bunched beam leading to additional gas desorption and heat loads on the cryogenic system, (iii) create secondary electrons which may contribute to electron multipacting [2,4,7]. This latter phenomenon is a resonant effect where a cloud of secondary electrons oscillate, in phase with the bunched beam, between opposite walls of the vacuum chamber, which may eventually limit LHC performance. The former manifestations of an electron cloud have been observed in the low energy positron rings of the B-factories (KEKB, PEP II) [6] and the super proton synchrotron (SPS) [7,8]. In the B-factories the seed of electrons is dominated by photoelectrons created by synchrotron radiation (SR), in the SPS by residual gas ionisation. Those observations suggest that e-cloud related problems may be expected to occur at LHC, where photoelectrons will indeed be present.

In the arcs, synchrotron radiation with a beam divergence of 0.55 mrad for 5 eV photons will illuminate the beam screen at a mean incidence angle of 4.5 mrad. Specular photon reflection from perfectly smooth surfaces, at such energies and incidence angles, might be expected to be close to 100% [9]. Calculations at a given angle of incidence, predict that the low energy photons (VUV) are reflected more readily than the higher energy photons (soft X-ray). Photons in the UV energy range can be reflected significantly from polished surfaces even when impinging at near normal incidence. Real surfaces with a finite roughness are far from being perfect reflectors in the VUV and a certain percentage of the incident photons will be adsorbed and/or diffused.

Therefore, one may speculate that a significant intensity of diffusely scattered UV light exists from a real surface. Experiments using monochromatic light are required to measure the photon reflection to produce a realistic estimate of the intensity and spectral distribution of the reflected and/or diffusely scattered photons. Moreover, it is expected [9] that the spectrum of reflected and/or diffused white light (WL) will not resemble that emitted by the beam, but will be more skewed toward the low energy. Finally, if a significant number of photoelectrons are created by reflected and/or diffused photons, such photoelectrons will not necessarily be created simultaneously with the proton beam bunch passing. Their relevance, depending on their number, should be addressed in the BIEM codes where the photoelectrons are presently created synchronously with the passage of the proton beam.

The study of photon distribution is important, not only as emitted from the proton beam (SR), but also after different reflections, which will occur in the vacuum pipe. A very important fact is the presence, in the arcs, of a magnetic field of 8 T perpendicular to the orbit. The electrons photoemitted on the orbital plane will be constrained by the magnetic field to move along the field lines, thus they will not be able to cross the vacuum chamber, and gain energy from the beam. On the other hand, an electron emitted perpendicular to the orbital plane (hence parallel to the magnetic field) will only spiral along the field lines, participating more efficiently to secondary electron production and, eventually, to multipacting. This simple reasoning implies that it will be extremely beneficial to adsorb most of the SR on the orbit plane, where the created electrons cannot participate in the multipacting, rather than having them reflected on the top and bottom parts of the beam pipe. To this end, the LHC beam pipe has been designed and produced with a ''saw-tooth'' structure on the equator where the photons first impinge, so as to offer to such a grazing incident SR a close to normal incidence impact, hence reducing its reflectivity. Indirect measurements performed at CERN [10] and at BINP, Novosibirsk [11] on such saw-tooth chambers, with 40 μm high and 500 μm pitch, clearly indicate a strong reduction in the forward reflectivity, as desired, so that this structure is now part of the base-line design of the machine. The existing measurements give only an estimate of the reduction (increase) in the forward (diffuse)

reflectivity, but they do not give any insight on the energy distribution of the reflected photons. This work aims at studying the photon reflectivity for energies between 8 and 200 eV from industrial materials that will be used in the construction of the beam screen for LHC arcs. To correctly simulate the effect of SR emitted by the beam, a quantitative estimate in energy and number of the photons producing photoelectrons has been made.

2. Experimental

The samples studied were all part of the final production of co-laminated copper on stainless steel for the LHC beam screen (BS), including all cleaning stages, and surface preparation (both for the flat and the saw-tooth surface). One half of the analysed sample was flat while the other presents the saw-tooth structure. This double structured sample allowed one to directly compare the two surfaces, in identical experimental conditions.

The reflectivity measurements were performed at the BEAR beamline at ELETTRA in Trieste. This is a bending magnet beamline, which can provide a monochromatic beam with energies from 8 to 1400 eV with a resolving power between 2200 and 5800 [12], and a white light with a spectral distribution similar to that of the LHC (where the critical energy of the photon spectrum is 44 eV).

The experimental chamber provides five degrees of freedom for the positioning of the sample. It is equipped with an electron analyser and two photon detectors, mounted on a two rotation axes goniometer. A schematic view of the experimental set-up, together with the description of the available rotation axes and translation movements, is presented in Fig. 1. With the described configuration it was possible to measure incident light directly on the sample, the forward scattered and the diffused light. Light impinged onto the sample with 26 mrad incidence angle, the smallest grazing angle obtainable to guarantee full sample illumination within the experimental set-up used. A tungsten mesh, calibrated with the directly illuminated photon detector, was used to constantly measure the incoming flux.

The photon detector used was a photodiode AXUV100 by IRD. It provides good response and linearity in the employed energy range. The detector active surface is 10 mm × 10 mm and it could rotate along Θ_A and Φ_A keeping a constant distance to the sample of about 70 mm. In this geometry, the light collected at each photodiode position is the one emitted in a 8° × 8° solid angle. The set-up allows to determine the space distribution of the scattered light by computer controlled movements of the

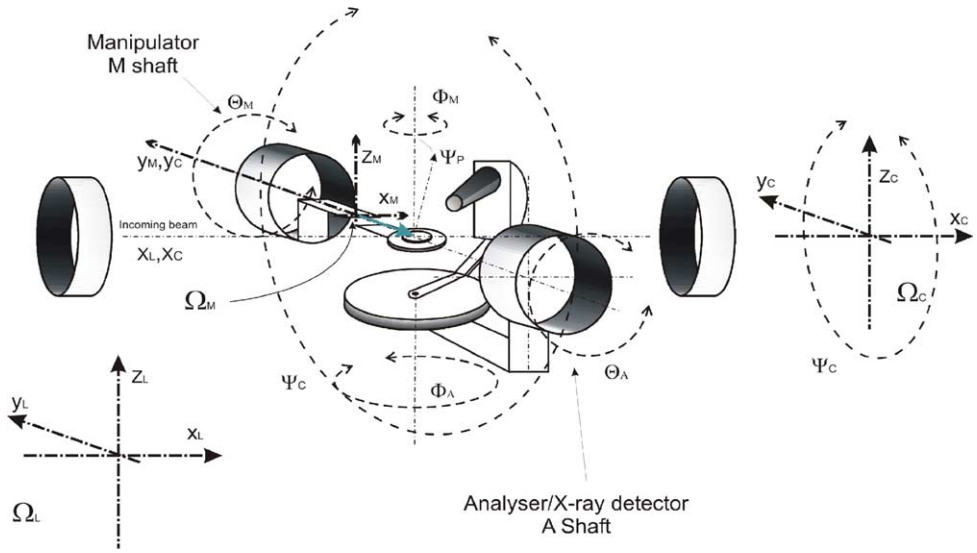

Fig. 1. Schematic view of the experimental set-up showing the degrees of freedom for the positions of the sample and of the photon detector.

detector over the entire space above the sample with the exception of the small region (close to $\Theta_A = 180^\circ$ and $\Phi_A = 0^\circ$) where the diode would have intercepted the incoming light. The complete solid angle above the sample has been divided in three different regions: the forward scattering region, $8^\circ \times 8^\circ$ around the centre of the geometrical reflection, the back-scattered region, $36^\circ \times 36^\circ$ around the incoming light direction; the diffused region which sums up all the emitted photons outside the two aforementioned regions. Such separation, although useful to analyse the data and their impact to the study of LHC–BIEM related simulations, is somehow artificial and is made considering experimental constraints such as the photodiode physical dimensions and the expected spread and beam divergence.

3. Results and discussion

In the first part of the experiment, the grating on the beamline was used as an inefficient mirror, which produced white light with a spectral distribution similar to that of LHC.

In Fig. 2, the photon reflectivity as a function of the azimuthal position Θ_A of the photodiode on the scattering plane is shown. The blue box shows the reflectivity of the as-received flat Cu sample, while the red box shows the data collected on the saw-tooth Cu sample. Each box represents a single measurement of the drain photocurrent measured by the diode (which covers 8° in the azimuth angle of the scattering plane) and normalised to the incident light. In case of the flat Cu surface, most (80%) of the reflected light is collected by the photodiode when placed around the geometrically defined specular (i.e. forward) direction and only a very small part of the incident light is back reflected or diffused (<2%). Probably part of the diffused component, being measured close to forward reflection, is produced by the intrinsic divergence of the reflected beam due to the roughness of the sample surface. These data are in agreement with previous measurements [13,14]. The sum of all the measured reflectivity, with the photodiode spanning over the whole solid angle above the irradiated flat Cu sample, allow us to extract the total reflectivity of 82% i.e., 18% of the incoming light is absorbed.

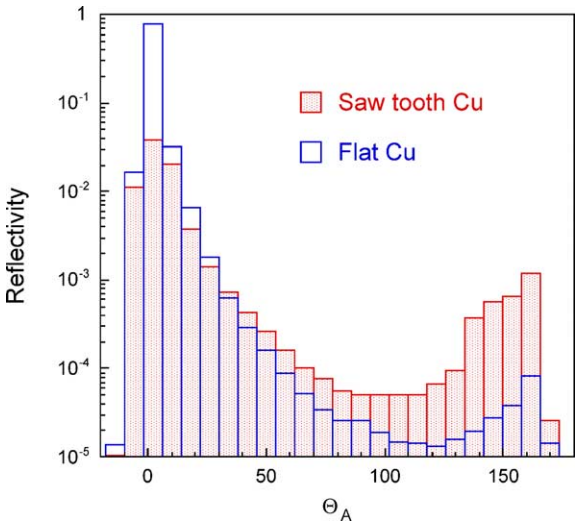

Fig. 2. Measured reflectivity, on the scattering plane, from a flat Cu sample (blue empty bars) and from the saw-tooth sample (red bars). Each point measure the reflectivity collected by the diode (whose angular dimension in the scattering plane was 8°).

On the other hand, the forward scattering measured from the saw-tooth sample is only about 4% while the total reflectivity, over the entire space, is around 10% i.e., 90% of the incoming light was absorbed. This also agrees with previous experiments [10,11]. The residual forward scattering reflectivity of the saw-tooth structure may be explained by the presence of flat surface in the ''crest'' of the saw-tooth, which essentially act as the flat sample, but with a reduced active surface. The diffused and back-scattered components, on the other hand, are due to persistent reflectivity even close to normal incidence, as expected theoretically. Also in this case the diffused component measured closer to the geometrical specular reflection is probably due to a significant increase in beam divergence of the reflected beam caused by roughness and imperfection of the saw-tooth structure surface.

From the available data, the values of the measure white light reflectivity in the two cases studied are given in Table 1.

The reduction of the total number of reflected photons by using the saw-tooth structure is significant, and only apparently increases the light diffused or back-scattered. Given the horizontal and vertical divergence of the beam impinging on the wall, if no saw-tooth structure were foreseen, the vacuum chamber would be evenly illuminated by the forward

Table 1
Measured values of the forward scattering, back scattering and diffused light expressed in percentage of the incoming light

	Flat sample	Saw-tooth sample
Forward scattering (%)	80	4
Back scattering (%)	0	2
Diffused (%)	2	4
Total	82	10

reflected light after a few reflections, giving a diffused photon background between 40 and 60%, that is much higher than that resulting from back and diffused scattering from the saw-tooth structure.

In order to determine the spectral composition of the reflected light, measurements have been performed with monochromatic light. The chosen photon energies were spanned in the range 8–200 eV. The dependence of the reflectivity of the analysed samples versus photon energies is shown in Fig. 3. The three curves represent the spectral distribution when the diode was placed: (i) on the geometrical specular reflection, to measure the photon energy dependence of the forward scattered light (black line); (ii) as close as possible to the impinging light direction (on the azimuth plane and with $\Theta_A = 162^\circ$), where the saw-tooth structure showed a maximum in the back-scattered light intensity (see Fig. 2) to measure its energy dependence; (iii) and with the photodetector on the scattering plane along the normal to the sample surface, to measure the energy variation of reflectivity in a representative position where diffused light is expected (green line). The blank intervals in the plots of Fig. 3 are due to the presence, in some of the data collected, of electrical noise that was dominating the physical information. Such data points have been rejected, without affecting the overall information presented here. The forward reflectivity of both the Cu co-laminated flat and the saw-tooth sample, even if different in absolute value, is almost constant, i.e., the spectral shape of the forward reflected electrons is very similar (up to 200 eV) to the one of the impinging photon energy distribution. This confirms that the origin of such component in the saw-tooth structure must be due to flat portions of the sample present in the "crest" of the saw-tooth. On the other hand, the diffused and back-reflected photons, have only quite low energies (below 20 eV), confirming that they derive from close-to-normal incidence reflectivity on the saw-teeth, or on high-angle scattering due to imperfections on the flat Cu surface. At such high angles of incidence only low-energy photons are expected to be significantly reflected. The implication of these observations in terms of expected number of photoelectrons produced by the reflected light is extremely important. Not only, the saw-tooth structure decreases the number of photoelectrons produced simply due to the close to normal incidence photon illumination, but also to the reduced energy of the photons reflected by its structure. The first mechanism for photoemission reduction is simply based on the fact that close to normal incidence photons have less probability to create a photoelectron close to the surface region, where electrons can escape into the vacuum. Photons impinging with a very grazing angle, on the other hand, travel further in the close-to-the-surface region, hence have a higher probability to produce photoelectrons. The second mechanism is related to the strong absorption of photons with energy higher than 20 eV from the saw-tooth structure. Low-energy photons are obviously less efficient in producing a secondary cascade within the solid, hence inducing photoelectrons emission. Even if the photoelectron distribution over the entire space in both cases, needs to be experimentally studied with greater

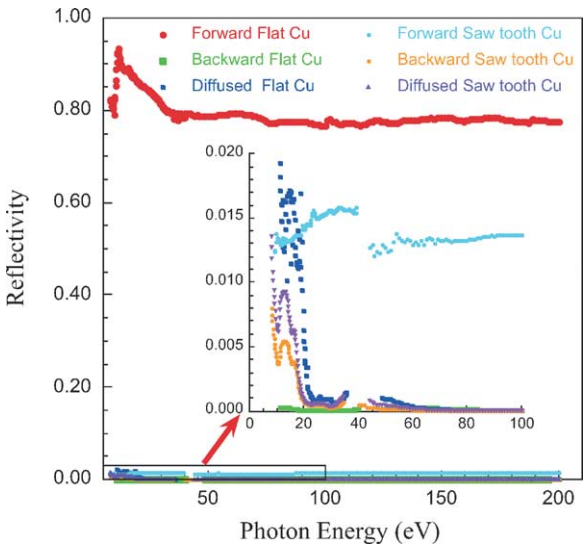

Fig. 3. Reflectivity of the measured flat and saw-tooth Cu surface vs. impinging monochromatic photon energy between 8 and 200 eV.

detail, our data imply that from an industrially prepared flat Cu surface one expects a high reflection of high-energy photons (between 20 and 200 eV) which can create a significant number of photoelectrons. On the other hand, in the case of the saw-tooth sample, we measured a reduced reflectivity, mainly of low-energy photons which will not significantly participate to the creation of photoelectrons as compared to the high-energy ones [3].

4. Conclusions

With these reflectivity measurements not only we confirmed the measurements on the forward reflectivity previously performed [10,13,14] or preliminary measurements of diffuse reflectivity [11], on the Cu flat and saw-tooth co-laminated sample but we also quantified the reflectivity in backwards and diffused directions.

The measurements performed with monochromatic light allowed the determination of the spectral distribution of the reflected/diffused light. It is demonstrated that, in the case of the saw-tooth sample, the back-reflected and diffused light consist almost entirely of low-energy photons, while the forward-scattered light has an energy distribution very similar to that of the flat sample, indicating, as expected, that this sample behaves in forward direction as a very low efficiency flat mirror surface.

Considering the beam divergence in the closed system of the LHC, the saw-tooth structure reduces the number of photons impinging on the wall synchronously to the proton beam (the forward reflected photons) by more than a factor 20, and significantly reduces the diffused light, which in the saw-tooth case mainly derive from back-scattered photons, while in the flat surface case, would derive from multiple reflections of the naturally divergent forward-scattered beam. Our data confirm the validity of the adopted solution for LHC arcs beam screen and produce quantitative estimates of photon reflectivity to be used in BIEM calculation.

Acknowledgements

The authors are indebted to N. Hilleret, and P. Strubin for fruitful discussions. The authors thanks ELETTRA and BEAR team for continuous support and assistance.

References

[1] J. Gómez-Goñi, O. Gröbner, A.G. Mathewson, J. Vac. Sci. Technol. A 12 (4) (1994) 1714.
[2] O. Gröbner, Vacuum 47 (6–8) (1996) 591;
O. Gröbner, PAC proceedings, Vancouver, 1997.
[3] R. Cimino, V. Baglin, I.R. Collins, Phys. Rev. Special Top.: Accelerators Beams 2 (1999) 063201.
[4] F. Zimmermann, in: Proceedings of the ECLOUD'02, CERN, Geneva, April 15–18, CERN-2002-001, 2002.
[5] J.M. Jimenez, et al., CERN-LHC Project Report 632, 2003.
[6] H. Fukuma, in: Proceedings of the ECLOUD'02, CERN, Geneva, April 15–18, CERN-2002-001, 2002.
[7] J.M. Jimenez, et al., in: Proceedings of the PAC 03.
[8] B. Henrist, N. Hilleret, M. Jimenez, C. Scheuerlein, M. Taborelli, G. Vorlaufer, in: Proceedings of the ECLOUD'02, CERN, Geneva, April 15–18, CERN-2002-001, 2002.
[9] http://www-cxro.lbl.gov/optical_constants/and references therein.
[10] V. Baglin, et al., Chamonix 11 (2001).
[11] V.V. Anashin, I.R. Collins, R.V. Dostovalov, N.V. Federov, O. Gröbner, A.A. Krasnov, O.B. Malyshev, E.E. Pyata, Vacuum 60 (2001) 255–260.
[12] http://bear.tasc.infm.it.
[13] V. Baglin, I.R. Collins, O. Gröbner, in: Proceedings of the EPAC'98, Stockholm, June 1998.
[14] V.V. Anashin, O.B. Malyshev, N.V. Federov, V.P. Nazmov, B.G. Goldenberg, I.R. Collins, O. Gröbner, Nucl. Inst. Meth. Phys. Res. A 448 (2000) 76–80.